J. Indian Chem. Soc.,
Vol. 88, October 2011, pp. 1483-1492

Synthesis and characterization of axially ligated zinc(II)-*para*-nitro-*meso*-tetraphenylporphyrin

Gauri D. Bajju*, Sujata Kundan and Sunil Kumar Anand

Department of Chemistry, University of Jammu, New Campus, Baba Sahib Ambedkar Road, Jammu-180 006, Jammu & Kashmir, India

E-mail : gauribajju@gmail.com

Manuscript received 10 December 2010, accepted 09 March 2011

Abstract : Reaction of *p*-nitro-*meso*-tetraphenylporphyrin (*p*-NO_2-H_2TPP) with zinc(II) acetate ($Zn(OAc)_2$) and phenol result in the formation of corresponding axially ligated zinc(II)-*p*-nitro-*meso*-tetraphenylporphyrin (X-Zn^{II}-*p*-NO_2TPP) (where X = axial phenolic ligands and TPP = tetraphenylporphyrin). The four-coordinated zinc porphyrin will accept one and only one axial ligand in 1 : 1 molar ratio to form five-coordinated complexes (Fig. 1), which are purified by column chromatographic method and characterized by UV/Vis, IR, NMR, Mass and elemental analysis. The visible spectra of the compounds in different solvents show a red shift (bathochromic shift) which increases in the magnitude depending upon the charge and polarizability of the axial ligation to Zn-*p*-NO_2TPP but not on the strength of the zinc ligand bond. The IR spectra show the appearance of metal-nitrogen (Zn-N) and metal-ligand (Zn-X) vibrations. The ^{1}H NMR results in $CDCl_3$ indicate the merging of protons of the phenolic ring axially attached to the central metal ion with that of the tetraphenyl ring of the Zn-*p*-NO_2TPP. The Mass spectra show that the molecular weight of the porphyrin agree well with the calculated *m/z* values. The elemental analysis shows the percentage of various elements in the compounds formed.

Keywords : *p*-Nitro-*meso*-tetraphenylporphyrin, zinc-porphyrins, oxygen donors, spectroscopic studies.

Introduction

Porphyrins and metalloporphyrins are essential to the life of bacteria, fungi, plants and animals, and have received considerable attention from many investigators in various fields. Porphyrins are used, for example, to mimic the function of hemeprotein such as cytochrome P_{450} in oxidation catalysis[1], as photosensitizers in photodynamic therapy of cancer (PDT)[2], in electron transport chains[3] and as building blocks in molecular devices[4]. Oxometalloporphyrin species are used to initiate the polymerization of propylene oxide, β-propiolactone and β-butyrolactone giving oligoethers and oligoesters having narrow molecular weight distribution[5]. Synthetic porphyrins are also used as fluorescent indicators for the delineation of neoplastic tissue in cancer patients. In the past, it was found that such compounds might be used as tumor selective radiation sensitizers and were used in cancer therapy[6-9]. Each research area requires porphyrins with different and specific structural features, bearing a variety of different substituents. The *para*-nitro groups are important, since they remove electron density from the porphyrin ring and provide steric hindrance improving the stability of the metalloporphyrin to act as catalysts in oxidation reaction and as radio sensitizers[10]. Actually, much attention has been paid to porphyrin containing magnesium(II), tin(IV) or rhodium(III) as metal centers[11].

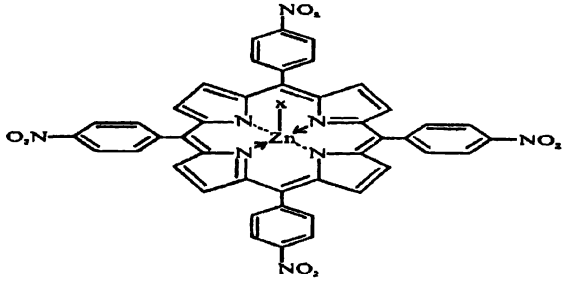

X = Oph;
α-, β-napthol
o-, *m*-, *p*-NH_2Oph
o-, *m*-, *p*-OCH_3Oph
o-, *m*-, *p*-NO_2Oph
o-, *m*-, *p*-ClOph
2,4-dichlorophenol

Fig. 1. Structure of axialy ligated zinc(II)-*p*-methyl-*meso*-tetraphenylporphyrin.

Although stable complexes of zinc(II) porphyrins are well known which result from the formation of four equivalent σ bonds N→M, that is filling of vacant *S*, P_x, P_y and $(n - 1)d_{x^2-y^2}$ or $nd_{x^2-y^2}$ orbitals of the cation with σ-electrons of the central nitrogen atoms. The axial coordination on the metal centre is a powerful synthetic way to synthesize large multiporphyrinic system[12] and the zinc(II) porphyrin possesses a tightly bound ligand, the nature of which influences the photophysical properties depending upon the spin-orbital coupling character of the ligand. The oxygen derivatives of zinc(II)-*p*-nitro-*meso*-tetraphenylporphyrin represent the supra-molecular binding motif, which finds applications for the construction of molecular square, coordination polymers, and other types of structure[13]. During the course of reaction studies of axial ligated zinc(II) derivatives, we observe substantial spectral shifts of the electronic absorption spectrum as a function of the nature of axial ligands. Although such effect have been observed previously for a limited range of ligands[14–17], we have extended the range of ligands and studied these spectra more deeply because zinc porphyrin complexes are simpler system in which metal is in +2 oxidation state, the four-coordinate zinc porphyrin will accept one and only one axial ligand[18–20] to form five-coordinated complexes and since, the electronic configuration is d^{10}, there are no empty *d*-orbital involved in the bonding.

In the present study, we report the synthesis of axially ligated zinc(II)-*p*-nitro-*meso*-tetraphenylporphyrin and their structural assignment by various spectroscopic techniques in order to understand the variation in porphyrin ring substituent, central metal ion and axial ligation with the porphyrin.

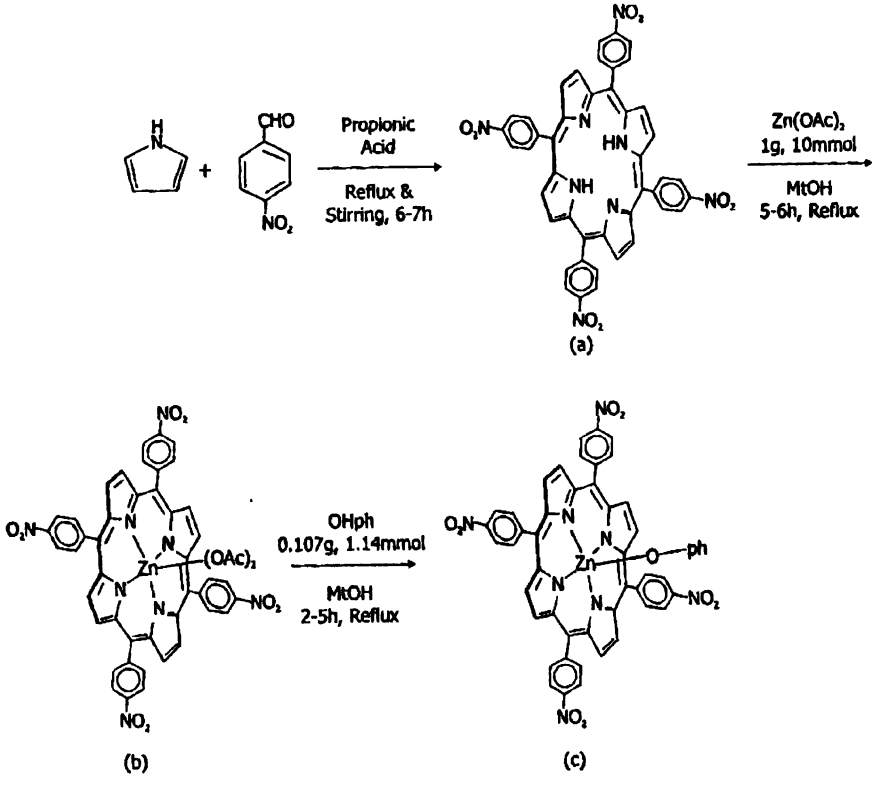

Scheme. 1. Schematic representation for the synthesis of (a) *p*-nitro-*meso*-tetraphenylporphyrin, (b) *p*-nitro-*meso*-tetraphenylporphyrin zinc(II) and (c) axially ligated zinc(II)-*p*-nitro-*meso*-tetraphenylporphyrin.

Experimental

Materials and methods :

All the solvents employed in the present study were of AR grade and were distilled before use. *p*-Nitrobenzaldehyde and pyrrole were distilled over KOH pellets under reduced pressure before use. Aluminium

oxide (basic), zinc(II) acetate ($Zn(OAc)_2$) were purchased from E. Merck, India. The various phenols used as axial ligand were of AR grade and obtained from Himedia and Sisco Research Laboratories Pvt. Ltd. and were used in the same state as received. Basic alumina oxide (200–300 mesh) and silica gel 60 (100–230 mesh) was used for column chromatography.

UV-Visible spectra were collected on Hitachi UV-3400, Lambda 35 UV/Vis spectrophotometer using different solvents. The spectra were recorded in 10 mm path length quartz cells (Hellma). The oscillator strength (*f*) of the compound was calculated from the expression, $f = 4.33 \times 10^{-9}\ \varepsilon\Delta\nu_{1/2}$, where ε is the molar absorption coefficient in $dm^3\ mol^{-1}\ cm^{-1}$ and $\Delta\nu_{1/2}$ is full width at half maximum in cm^{-1}. Infrared spectra were recorded on Perkin-Elmer spectrophotometer. The nuclear magnetic resonance spectra were recorded on Bruker Avans 400 MHz spectrometer using tetramethylsilane (TMS) as internal standard. Mass spectra were obtained on Bruker Daltonic Mass spectrophotometer using chloroform. Elemental analysis was carried out on Perkin-Elmer (CHNS-932) elemental analyzer.

Results and discussion

Absorption spectroscopy :

The electronic absorption spectra of porphyrins proper are characterized by complexity, variability of the band position and intensity as a function of structure, low molar extinction coefficient (ε) of the visible bands, high intensity of the soret bands, and low sensitivity of the bands to the nature of the inert solvents. It may be noted that free base porphyrins (H_2TPP) exhibit four Q-banded spectrum in visible region whereas, metalloporphyrins exhibit only two Q-bands because metal ion behaved as Lewis acids accepting lone pairs of electron from dianionic porphyrin ligand and also, upon metal incorporation, the symmetry of the porphyrin increases to D_{4h} from D_{2h} in free-base porphyrins resulting in the appearance of two Q-banded spectra.

During reaction study of axially ligated Zn^{II}-*p*-NO_2TPP, it was observed that there is substantial spectral shift of electronic absorption and have low magnitude of oscillator strength relative to their free-base porphyrins due to the presence of various phenolic ligands attached to Zn^{II}, which alters the orbital energies relative to the free-base porphyrins. Three effects are seen upon addition of axial ligands : (i) a red shift of the entire spectrum relative to that of ZnTPP, (ii) a change in the relative intensities of the α- and β-bands, that is correlated with the magnitude of the red shift and (iii) the magnitude of the red shift is shown to depend on the charge and polarizability of the axial ligand but not on the strength of the zinc-ligand bond indicating a large electrostatic contribution to the binding of ligand to Zn-*p*-NO_2TPP. The red shift and α, β intensity ratio changes derive from the amount of negative charge transferred from the ligand to the porphyrin ring via the zinc atom. It is of interest to note that among the different axial ligands attached to metal ion, those having electron donating axial ligands have broadened soret and visible bands and are slightly bathochromic while those having electron withdrawing axial ligands attached to metal have hypsochromic B- and Q-bands (Table 1). It was also observed that only marginal change in λ_{max} values, absorption coefficient (ε) and oscillator strength (*f*) values were observed among different solvents inferencing that change in po-

Table 1. Optical absorption data of X-Zn-*p*-NO_2TPP in chloroform showing the λ_{max} together ε and half width of the spectral transition ($\nu_{1/2}$)

No.	Compd.	B-band λ_{max} (log ε), $\nu_{1/2}$ (nm) ($M^{-1}\ cm^{-1}$), (cm^{-1})	Q-band λ_{max} (log ε), $\nu_{1/2}$ (nm) ($M^{-1}\ cm^{-1}$), (cm^{-1})
1.	*p*-NO_2-H_2TPP	418, (0.421), 710	517, (0.52), 613 550, (0.036), 617 589, (0.029), 619 645, (0.027), 620
2.	Zn-*p*-NO_2TPP	425, (0.48)	547, (0.11) 583, (0.056)
3.	phO-Zn-*p*-NO_2TPP	420, (0.031), 700	548, (0.111), 611 583, (0.057), 431

Table-1 (contd.)

4.	α-phO-Zn-*p*-NO_2TPP	421, (0.026), 740	546, (0.118), 647 581, (0.049), 462
5.	β-phO-Zn-*p*-NO_2TPP	421.5, (0.479), 895	545, (0.121), 650 579, (0.036), 436
6.	*o*-OCH_3phO-Zn-*p*-NO_2TPP	424, (0.554), 918	547, (0.123), 614 581, (0.028), 405
7.	*m*-OCH_3phO-Zn-*p*-NO_2TPP	424, (0.553), 866	547, (0.227), 676 584, (0.134), 456
8.	*p*-OCH_3phO-Zn-*p*-NO_2TPP	424, (0.554), 866	547, (0.249), 614 581, (0.114), 483
9.	*p*-NH_2phO-Zn-*p*-NO_2TPP	423, (0.524), 846	547, (0.638), 609 582, (0.592), 460
10.	*o*-NH_2phO-Zn-*p*-NO_2TPP	423, (0.522), 947	547, (0.512), 707 581, (0.124), 462
11.	Cl_2phO-Zn-*p*-NO_2TPP	423.5, (0.882), 988	541, (0.856), 627 575, (0.324), 471
12.	*o*-ClphO-Zn-*p*-NO_2TPP	422, (0.672), 905	546, (0.469), 709 587, (0.112), 452
13.	*m*-ClphO-Zn-*p*-NO_2TPP	422, (0.678), 853	546, (0.314), 616 587, (0.262), 425
14.	*p*-ClphO-Zn-*p*-NO_2TPP	422, (0.672), 956	546, (0.874), 709 587, (0.394), 449
15.	*o*-NO_2phO-Zn-*p*-NO_2TPP	421.9, (0.476), 906	545, (0.964), 650 586, (0.684), 454
16.	*m*-NO_2phO-Zn-*p*-NO_2TPP	421.5, (0.466), 861	546, (0.764), 616 586, (0.584), 426
17.	*p*-NO_2phO-Zn-*p*-NO_2TPP	421, (0.432), 939	545, (0.624), 650 581, (0.584), 462

larity of solvents does not significantly alter the position of the transitions but results in enhanced $\nu_{1/2}$ values indicating weak interaction with the solvents and the magnitude of the red shift (bathochromic) of Q-bands depend upon the polarity of the solvent and was increased with the decreased in polarity. The optical absorption spectra of the free-base compound and its axially ligated Zn^{II} derivatives were recorded in different solvents (Table 2)

Table 2. Optical absorption data of X-Zn-*p*-NO_2TPP in different solvents

No.	Compd.	Solvents	B-band λ_{max} (log ε), $\nu_{1/2}$ (nm) (M^{-1} cm^{-1}), (cm^{-1})	*f*-value B-band	Q-band λ_{max} (log ε), $\nu_{1/2}$ (nm) (M^{-1} cm^{-1}), (cm^{-1})	*f*-value Q-band
1.	phO-Zn-*p*-NO_2TPP	$CHCl_3$	420, (0.031)	0.0020	548 (0.111) 583 (0.051)	0.0004
		CH_2Cl_2	417, (0.526)	0.1138	548.76 (0.224) 586.327 (0.0351)	0.0012
		CCl_4	424 (0.935)	0.0110	549.31 (0.390) 588.371 (0.0785)	0.0021
		Toluene	426 (0.409)	0.0029	548.310 (0294) 589.374 (0.049)	0.0003

Table-2 (contd)

2.	*p*-NH_2phO-Zn-*p*-NO_2TPP	$CHCl_3$	423 (0.524)	0.0192	547 (0 638) 582 (0 592)	0 0005
		CH_2Cl_2	420 (0.546)	0.0188	546.21 (0 225) 581 132 (0 054)	0 0016
		CCl_4	424 (0 321)	0.0580	548.143 (0 224) 585 118 (0 045)	0 0061
		Toluene	425 (0.482)	0 0484	549 212 (0 185) 586 015 (0 032)	0 0009
3.	*p*-NO_2phO-Zn-*p*-NO_2TPP	$CHCl_3$	422 (0.432)	0 0035	545 (0.624) 581 (0 584)	0 0075
		CH_2Cl_2	419 (0.431)	0.0030	544 184 (0.223) 580.147 (0 048)	0 0003
		CCl_4	421 (0.316)	0.0024	546 301 (0.225) 584 731 (0.32)	0 0013
		Toluene	423 (0.414)	0.0010	548.432 (0.252) 584.196 (0 212)	0 0015
4.	*p*-OCH_3phO-Zn-*p*-NO_2TPP	$CHCl_3$	424 (0 554)	0.0052	547 (0.249) 581 (0.114)	0 0017
		CH_2Cl_2	420 (0.325)	0.0029	547.831 (0.346) 584.213 (0.321)	0 0024
		CCl_4	425 (0.386)	0.0037	547.943 (0.427) 584.326 (0 327)	0 0121
		Toluene	426 (0 3472)	0 0037	547 742 (0 984) 584 432 (0 247)	0.0020

and spectra are displayed in Fig. 2. For example, in *p*-NH_2PhO-Zn-*p*-NO_2TPP, λ_{max} values in $CHCl_3$ were observed at 423, 547, 582 nm while in CCl_4 and toluene the λ_{max} values were observed at 424, 548, 585 nm and 425, 549, 586 nm respectively. However, B (0,0) exhibits only a small change in the *f* value, but Q (0,0) band undergoes interesting changes in the nature of the solvent. The *f* value of Q (0,0) for *p*-NH_2PhO-Zn-*p*-NO_2TPP in $CHCl_3$, CH_2Cl_2, CCl_4 and toluene was observed at 0.0005, 0.0016, 0.0009 and 0.0075 respectively. The magnitude of change in *f*-values in different porphyrin shows the relative strength of $\pi \rightarrow \pi^*$ interaction.

^1H NMR spectra :

The ^1H NMR spectra of the axially ligated zinc(II) derivatives are helpful in establishing the structural integrity of the compounds. Representative spectra are shown in Fig. 3 (a and b) and Table 3 summarizes the data obtained for the various axially ligated porphyrins. The axially ligated porphyrins exhibit proton resonance characteristics of substituted *meso*-phenyl group, β-pyrrole and axially bound phenols. In case of free-base para-nitro-*meso*-tetraphenylporphyrin, the imino protons (N–H) resonate at –2.62 ppm since induced magnetic field generates strong shielding effect that causes a diamagnetic shift to upfield. However, it disappears in Zn-*p*-NO_2TPP which shows the coordination of porphyrin nitrogen with zinc atom. The effects of *meso*-substituent on the β-pyrrole protons have earlier been reviewed in literature[21]. For *p*-NO_2-H_2TPP, the β-pyrrole protons resonate at 8.69 ppm comparing to 8.84 ppm as in case of *meso*-tetraphenylporphyrin. This is due to electron withdrawing effect of the nitro groups at the *meso*-phenyl position, which leads to less deprotection by the anisotropy effect on these β-pyrrole hydrogens[22]. In case of α-phO-Zn-*p*-NO_2TPP (α-phO-α-naphthol), the β-pyrrole protons resonate as a singlet at 9.2 ppm and *meso*-aryl protons resonate as a singlet at 8.4 ppm for H_o and a doublet at 7.6 ppm for H_m. In comparison to this for *p*-NH_2phO-Zn-*p*-NO_2TPP (*p*-NH_2phO-*para*-amino phenol), the β-pyrrole proton resonate as a singlet at 8.6 ppm and

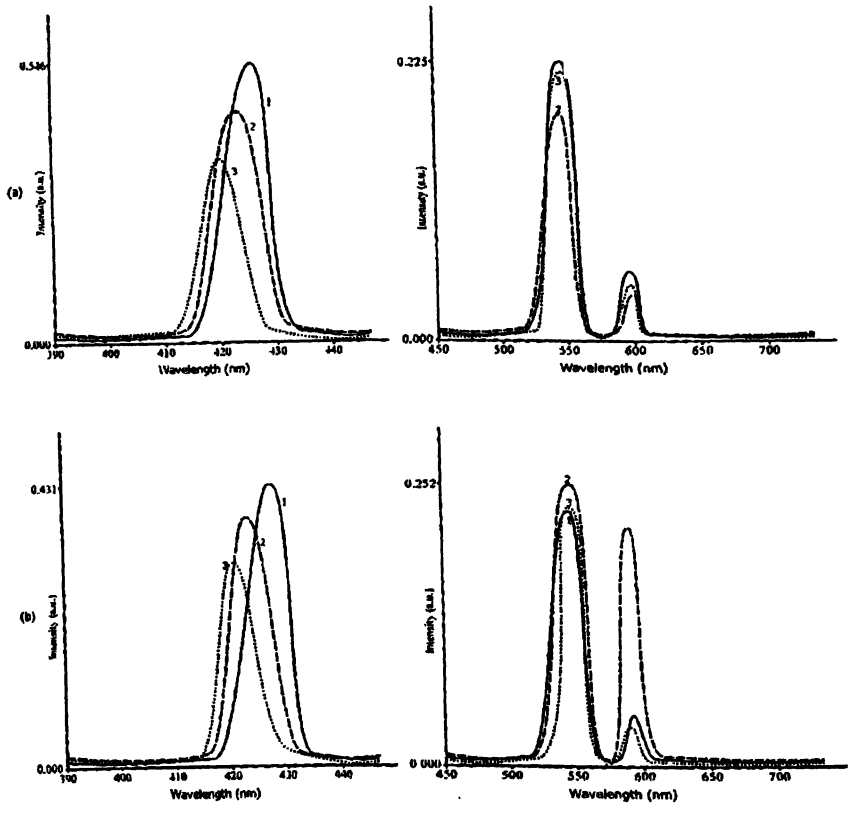

Fig. 2. Absorption spectra for (a) *p*-NH_2phO-Zn-*p*-NO_2TPP and (b) *p*-NO_2phO-Zn-*p*-NO_2TPP in different solvents : (1) dichloromethane; (2) toluene and (3) carbontetrachloride.

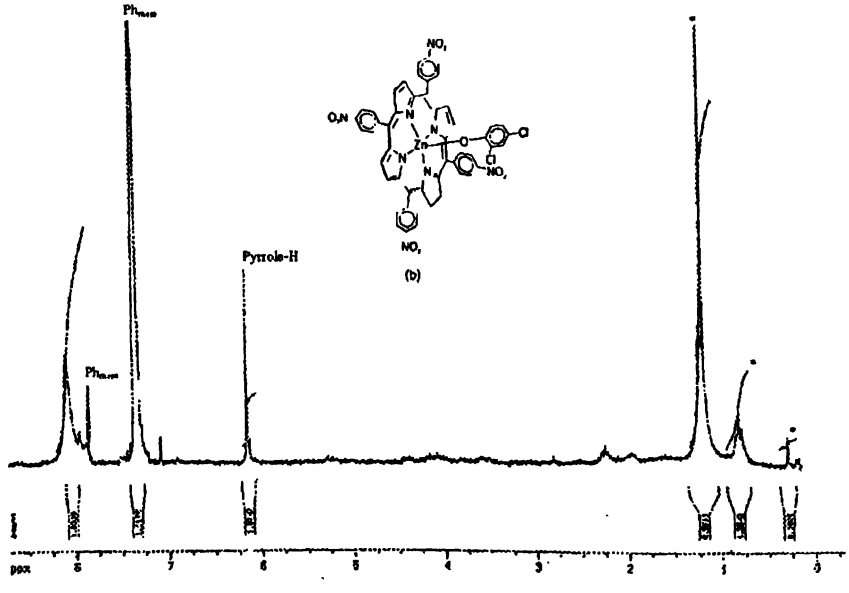

Fig. 3(a). ^1H NMR spectra of 2,4-Cl_2phO-Zn-*p*-NO_2TPP in $CDCl_3$ at 300 K. Starred peaks are solvents impurities.

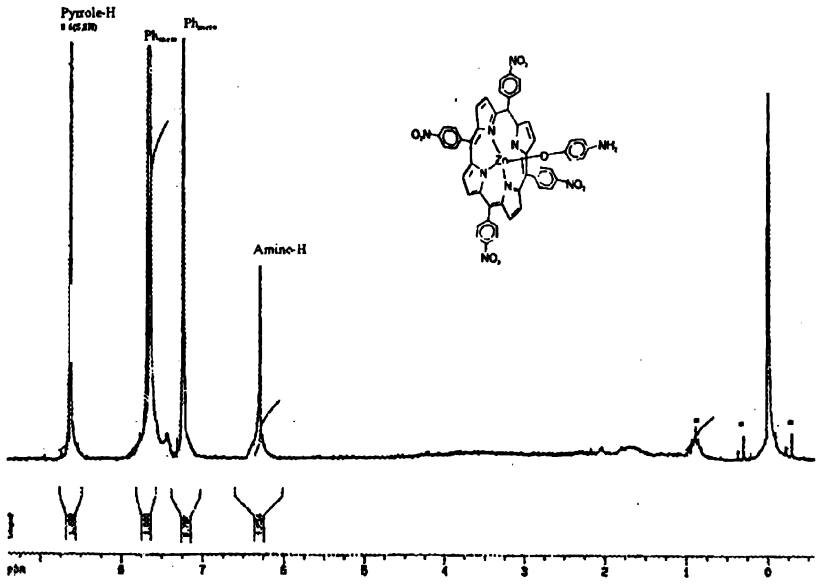

Fig. 3(b). ^{1}H NMR spectra of *p*-NH_2phO-Zn-*p*-NO_2TPP in $CDCl_3$ at 300 K. Starred peaks are solvents impurities.

Table 3. ^{1}H NMR data[a] showing chemical shifts (δ in ppm) values of the free-base and axially ligated Zn^{II}-*p*-NO_2TPP in $CDCl_3$

No.	Porphyrins	δ, ppm imino protons	δ, ppm β-pyrrole protons	δ, ppm *meso*-aryl protons	δ, ppm other protons
1.	*p*-NO_2-H_2TPP	-2.62 (2H, s)	8.69 (8H, s)	8.15 (8H, d, H_o)	
				7.48 (8H, t, H_m)	
2.	Zn-*p*-NO_2TPP		8.72 (8H, s)	8.14 (8H, d, H_o)	
				7.56 (8H, d, H_m)	
3.	α-phO-Zn-*p*-NO_2TPP		9.2 (s)	8.4 (10H, d, H_o)	
				7.6 (10H, d, H_m)	
4.	*p*-NH_2phO-Zn-*p*-NO_2TPP		8.6 (8H, s)	7.8 (10H, d, H_o)	6.2 (2H, s, H_{NH_2})
				7.2 (10H, d, H_m)	
5.	*o*-NH_2phO-Zn-*p*-NO_2TPP		8.8 (8H, s)	8.1 (10H, d, H_o)	6.5 (2H, s, H_{NH_2})
6.	*p*-OCH_3phO-Zn-*p*-NO_2TPP		8.9 (8H, s)	7.9 (10H, d, H_o)	3.8 (3H, s, H_{OCH_3})
				8.4 (10H, m, H_m)	
7.	2,4-Cl_2phO-Zn-*p*-NO_2TPP		6.2 (8H, s)	8.14 (9H, m, H_o)	
				7.43 (10H, d, H_m)	

[a]δ in ppm, the nature of splitting pattern(s) (s = singlet, d = doublet, t = triplet, m = multiplet), number of proton(s) and their location in the porphyrin spectra respectively are given in parenthesis; *o - ortho, p - para, m - meta.*

meso-aryl proton resonate as a doublet at 7.8 ppm (H_o) and 7.2 ppm (H_m). In addition to this, there was an extra peak as a singlet resonated at 6.2 ppm corresponding to the amino hydrogen of the phenol ring. It has been observed that there occurs a slight difference in the chemical shift value of *p*-NH_2phO-Zn-*p*-NO_2TPP and α-phO-Zn-*p*-NO_2TPP which is due to the electron releasing effect of (amino) NH_2 group of the phenol ring which shift the spectrum to the upfield causes shielding of the proton. The data also show that the proton of the phenolic ring axially attached to the central metal ion is merged with the protons of the phenyl ring of the porphyrin.

IR spectroscopy :

Infra-red absorption spectroscopy is an important and non-destructive characterizing tool, which provides qualitative information regarding structural detail of crystal material[23]. *p*-Nitro-*meso*-tetraphenylporphyrin containing the NO_2 group at *meso*-phenyl position show strong absorption bands from symmetric and asymmetric deformation (1389–1259 cm^{-1} and 1661–1499 cm^{-1} respectively)[24]. The exact position of these bands depend on the substitution and unsaturation within the NO_2 group involving symmetrical and asymmetrical stretching vibration at 1348 cm^{-1} and 1525 cm^{-1} respectively which agree with the Collman's *et al.*[25] results assigned to the NO_2 group for symmetrical and asymmetrical vibrations. The axially ligated Zn-*p*-NO_2TPP show the characteristic absorption bands for the *p*-NO_2 group, Zn–N and Zn–O stretching respectively. The Zn–O band stretch is usually occur in the range of 546–560 cm^{-1}. The axially ligated Zn^{II} derivatives cause a slight variation in the value of vibrational frequencies. For example, in the spectra of compound phO-Zn-*p*-NO_2TPP, there are ν(C–H) (680 cm^{-1}), ν(C=C) (1634 cm^{-1}), ν(C–N) (1095 cm^{-1}), vibrational stretching frequencies. The ν(Zn–N) and ν(Zn–O) stretching vibrational frequencies occur at 474 and 557 cm^{-1} respectively. In comparison to this, the compound *p*-OCH_3phO-Zn-*p*-NO_2TPP, there are ν(C–H) (686 cm^{-1}), ν(C=C) (1629 cm^{-1}), ν(C–N) (1099 cm^{-1}), ν(Zn–N) (489 cm^{-1}) and ν(Zn–O) (556 cm^{-1}). In this compound, there are additional ν(C–H) (2952 cm^{-1}), ν(C–H) (2920 cm^{-1}), $\nu(C\text{–}O\text{–}C)_{sym}$ (1018 cm^{-1}) and $\nu(C\text{–}O\text{–}C)_{asym}$ (1261 cm^{-1}) corresponds to the -OCH_3 group of the axially ligated phenol with the zinc atom. The other bands frequencies that are not assigned attributed to the vibration of the porphyrin ring and phenyl groups.

Mass spectroscopy and elemental analysis :

The mass spectra of several porphyrins and their metalloderivatives have been obtained by MALDI-Mass spectroscopy technique[26]. Mass spectra of porphyrins and their derivatives are best recorded at the lowest possible temperature (usually approx. 200–250 °C). The intensity of molecular ion in the mass spectra of porphyrin has also been used in the study of deuteration (as a general example of electrophilic substitution) of porphyrins, metalloporphyrins, and some reduced derivatives. Table 4 summarizes the mass spectra and elemental analysis data of axially ligated Zn^{II} derivates.

Synthetic procedures :

p-Nitro-meso-tetraphenylporphyrin [p-NO_2-H_2TPP] :

The *p*-NO_2-H_2TPP was synthesized by the condensation reaction between pyrrole (1.02 g, 0.015 mmol) and *p*-nitrobenzaldehyde (3.0 g, 0.015 mmol) in refluxing propionic acid solution (200 ml). The solution was refluxed and stirred for 6–7 h and allowed to cool at room tem-

Table 4. The mass spectral data showing molecular ion peak (*m/z*) and elemental analysis data of axially ligated Zn^{II} porphyrin

No.	Compd.	Formula	Molecular ion peak (*m/z*)		Elemental analysis (%) : Calcd. (Found)		
			Calcd.	Found	C	H	N
1.	*o*-NH_2phO-Zn-NO_2TPP	$C_{50}H_{30}N_9O_9Zn_1$	966.22	965.21	62.21	3.12	13.06
					(62.15)	(3.26)	(13.18)
2.	*m*-NH_2phO-Zn-NO_2TPP	$C_{50}H_{30}N_9O_9Zn_1$	966.22	965.27	62.21	3.12	13.06
					(62.19)	(3.29)	(13.22)
3.	*p*-NO_2phO-Zn-NO_2TPP	$C_{50}H_{28}N_9O_{11}Zn_1$	996.12	995.83	60.30	2.83	12.65
					(60.63)	(2.96)	(12.72)
4.	*m*-NO_2phO-Zn-NO_2TPP	$C_{50}H_{28}N_9O_{11}Zn_1$	996.12	995.94	60.30	2.83	12.65
					(60.75)	(2.92)	(12.83)
5.	Cl_2phO-Zn-NO_2TPP	$C_{50}H_{27}N_8Cl_2O_9Zn_1$	1020.15	1020.46	58.85	2.66	10.97
					(58.98)	(2.87)	(10.72)
6.	*m*-ClphO-Zn-NO_2TPP	$C_{50}H_{28}N_8Cl_1O_9Zn_1$	985.67	986.43	60.88	2.85	11.35
					(60.75)	(2.53)	(11.24)

perature. The mixture was then filtered and washed with water and methanol until the washing solution was colourless. The precipitate was then dried under vacuum and dissolved in the minimum amount of chloroform and chromatographed on a basic alumina column using chloroform as the eluent. The first band was collected and reduced by vacuum to produce purple crystals (Scheme 1(a)). *p*-NO_2-H_2TPP was characterized by UV/Vis ($CHCl_3$) λ_{max} (ε) (nm) : 425, 517, 550, 589, 645; ^{1}H NMR (TMS) δ ppm : -2.62 (2H, s, N-H pyrrolic), 8.69 (8H, s, β-pyrrole), 8.15 (8H, d, H_o, *meso*-aryl), 7.48 (8H, t, H_m, *meso*-aryl); HRMS (*m/z*) : [M^+] Calcd. for $C_{44}H_{26}N_8O_8$, 794.44; found, 794.49; elemental analysis (Calcd., found for $C_{44}H_{26}N_8O_8$) : C (66.51, 66.50), H (3.27, 3.25), N (14.09, 14.04).

Preparation of p-nitro-meso-tetraphenylporphyrin zinc(II) [Zn-p-NO_2TPP] :

614 g (1 mmol) of pure *p*-nitro-*meso*-tetraphenylporphyrin was dissolved in 50 ml of chloroform and add 1 g (10 mmol) of zinc(II) acetate dissolved in 25 ml hot methanol was added to it. The solution was refluxed for 2 h and the solvent was removed under reduced pressure. The resulting solid was dissolved in a minimum amount of chloroform and filtered to remove excess zinc(II) acetate. The filter cake was discarded. The solvent was removed under reduced pressure and the resulting solid was redissolved in a minimum volume of hot chloroform (approx. 50 ml), purified on a silica column eluting with chloroform. The (Zn^{II}-*p*-NO_2TPP) band should be yellowish purple and should elute first. The solid was recrystallised from chloroform and petroleum ether (Scheme 1(b)). (Yield 90%) UV/Vis ($CHCl_3$) λ_{max} (ε) (nm) : 425, 547, 583; ^{1}H NMR (TMS) δ ppm : 8.69 (8H, s, β-pyrrole), 8.15 (8H, d, H_o, *meso*-aryl), 7.48 (8H, t, H_m, *meso*-aryl); HRMS (*m/z*) : [M^+] Calcd. for $C_{44}H_{24}N_8O_8Zn_1$, 857.83; found, 857.94; elemental analysis (Calcd., found for $C_{44}H_{24}N_8O_8Zn_1$) : C (61.60, 61.54), H (2.79, 2.82), N (13.05, 13.09).

Axially ligated zinc(II)-p-nitro-meso-tetraphenylporphyrm [X-Zn-p-NO_2TPP] :

0.107 g phenol (1.14 mmol) dissolved in minimum quantity of methanol and was added to a solution of Zn-*p*-NO_2TPP (0.982 g, 1.14 mmol) dissolved in 15 ml of chloroform and the mixture was stirred for 2-5 h (Scheme 1(c)). After stirring, the mixture was extracted with 2 *N* NaOH solution and chloroform as an eluent. The organic layer was dried over anhydrous sodium sulphate and chromatographed on a basic alumina column using chloroform as eluent. The intense yellowish-green band was gradually separated and collected as the desired product IR spectra (KBr) ν (cm^{-1}) : 2964 for aromatic (C-H), 1634 (C=C), 1095 (C-N), 1521 $(NO_2)_{asym}$, 1344 $(NO_2)_{sym}$, 474 (Zn-N), 557 (Zn-O); HRMS (*m/z*) : [M^+] Calcd. for $C_{50}H_{29}N_8O_9Zn_1$, 950.89; found, 950.54; elemental analysis (Calcd., found for $C_{50}H_{29}N_8O_9Zn_1$) : C (63.15, 63.12), H (3.05, 3.09), N (6.87, 6.91).

References

1. (a) P. R. Ortiz de Montellano, "Cytochrome P-450 Structure, Mechanism and Biochemistry", 2n ed., Plenum Press, New York, 1995; (b) D. Dolphin, T. G Traylor and L Xie, *Acc. Chem. Res.*, 1997, **30**, 251.
2. (a) O. Gaud, R. Granet, M. Kaouadji, P. Krausz, J. C. Blais and G. Bolback, *Can. J. Chem.*, 1996, **74**, 481; (b) K. Driaf, R. Granet, P. Krausz, M. Kaouadji, F. Jhomasson, A. J Chulia, B. Verneuil, M. Spiro, J. C. Blais and G. Bolbach, *Can. J. Chem.*, 1996, **74**, 1550.
3. T. J. Arinura, *Synth. Org. Chem. Jpn.*, 1997, **55**, 557.
4. (a) J. S. Lindsey, S. Prathapan, J. E. Johnson and R W Wagner, *Tetrahedron*, 1994, **50**, 8941; (b) C. M. Drain, F. Nifiatis, A. Vasenko and J. D. Batteas, *Angew. Chem Int Ed.*, 1998, **37**, 2344; (c) M. G. H. Vicente, M. T Caneilla, C. B. Lebrilla and K. M. Smith, *Chem. Commun.*, 1998, 2355; (d) H. A. M. Biemas, A. E. Rowan, A. Verhoeven, P. Vanoppen, L. Latterini, J. Schnning, E. W. Meijer, F. C. Schryver and R. J. M. Nolte, *J. Am. Chem. Soc.*, 1998, **120**, 11054; (e) A. Osuka and H. Shimidzu, *Angew. Chem. Int. Ed. Engl.*, 1997, **36**, 135.
5. (a) V. F. Slagt, J. H. N. Reek, P. J. C. Kamer and P. W N. M. Van Leeuwen, *Angew. Chem. Int. Ed.*, 2001, **40**, 4271; (b) V. F. Slagt, P. J. C. Kamer, P. W. N. M. Van Leeuwen and J. N. H. Reek, *J. Am. Chem. Soc.*, 2004. **126**, 1526.
6. J. Winkelman, S. Rubenfeld and J. Mcafee, *J. Nuclear Medicine*, 1964, **5**, 462.
7. P. Kubat and J. Mosinger, *J. Photochem. Photobiol. (A)*, 1996, **96**, 93.
8. E. Zenkerich, E. Sagun, V. Knyukshtol, S. Alexander, M. Andrei, E. Olga, B. Kaymond and S. P. Songa, *J. Photochem. Photobiol. (B)*, 1996, **33**, 171.
9. A. Kawamura-Konishi, S. Neya, F. Norika and S. Homo, *Biochem. Biophys. Res. Commun.*, 1996, **225**, 537.

10. G. G. Meng, B. R. James and K. A. Skov, *Can. J. Chem.*, 1994, **72**, 1894 and references therein.

11. (a) For examples, see : J. K. M. Sanders, N. Bampos, Z. Clydewatson, S. L. Darling, J. C. Hawley, H. J. Kim, C. C. Mak and S. J. Webb, "In The Porphyrin Handbook", eds. K. M. Kadish, K. M. Smith and R. Guillard, Academic Press, New York, 2000, **3**, 1-48; (b) E. Stulz, S. M. Scott, Y. F. Ng, A. D. Bond, S. J. Teat, S. L. Darling, N. Feeder and J. K. M. Sanders, *Inorg. Chem.*, 2003, **42**, 6564.

12. (a) U. Michelsen and C. A. Hunter, *Angew. Chem. Int. Ed.*, 2000, **39**, 764; (b) R. A. Haycock, C. A. Hunter, D. A. James, U. Michelsen and L. R. Sutton, *Org. Lett.*, 2000, **2**, 2435; (c) A. Tsuda, T. Nakamura, S. Sakamoto, K. Yamaguchi and A. Osuka, *Angew. Chem. Int. Ed.*, 2002, **41**, 2817; (d) L. J. Twyman and A. S. H. King, *Chem. Commun.*, 2002, 910; (e) D. Furutsu, A. Satake and Y. Kobuke, *Inorg. Chem.*, 2005, **44**, 4460; (f) R. Takahashi and Y. Kobuke, *J. Org. Chem.*, 2005, **70**, 2745.

13. V. F. Slagt, P. W. N. M. Van Leeuwen and J. H. N. Reek, *Chem. Commun.*, 2003, 2474; (b) V. F. Slagt, M. Roeder, P. J. C. Kamer, P. W. N. M. Van Leeuwen and J. H. N. Reek, *J. Am. Chem. Soc.*, 2004, **126**, 4056.

14. J. Fajer, D. C. Borg, A. Forman, R. H. Felton, L. Vegh and D. Dolphin, *N. Y. Acad. Sci.*, 1973, **206**, 349.

15. G. C. Vogel and L. A. Searby, *Inorg. Chem.*, 1973, **12**, 936.

16. G. C. Vogel and J. R. Stahlbush, *Inorg. Chem.*, 1977, **16**, 950.

17. K. M. Kadish, L. R. Shicle, R. K. Rhodes and L. A. Bottomley, *Inorg. Chem.*, 1981, **20**, 1274.

18. G. H. Kirskey, P. H. Ambright and C. B. Storm, *Inorg. Chem.*, 1969, **8**, 2141.

19. (a) J. R. Miller and G. D. Dorough, *J. Am. Chem. Soc.*, 1952, **74**, 3977; (b) G. C. Vogel and L. A. Searby, *Inorg. Chem.*, 1973, **12**, 935.

20. J. Fajer, D. C. Borg, A. Forman, R. H. Felton, L. Vegh and D. Dolphin, *Ann. N. Y. Acad Sci.*, 1973, **206**, 349.

21. H. Scheer and J. Katz, "In Porphyrins and Metalloporphyrins", ed. K. M. Smith, Elsevier, Amesterdam, 1935, 399.

22. A. Marco, Schiavon, S. Lidia, G. Iwamoto Antonio, Ferreira, I. Yassuko, V. B. Maria, Zanoni and D. Marilda das, Assis, *Journal of Braz. Chem. Soc.*, 2000, **11**, 458.

23. H. Burger, "Spectroscopy of Porphyrins and Metalloporphyrin".

24. R. M. Silverstain, G. C. Bassier and T. C. Morril, "Spectrometric Identification of Organic Compounds", John Wiley and Sons, Inc, 3rd ed., 1974.

25. J. P. Collman, J. I. Brauman, K. M. Zoxee, T. R. Halbert, E. Bunnenberg, R. E. Linder, G. N. Lanar, J. D. Gaudio and K. Spartation, *J. Am. Chem. Soc.*, 1980, **102**, 4182.

26. R. C. Dougherty, "In Biochemical Applications of Mass Spectrometry", ed. G. R. Waller, Wiley, New York, 1972, 591.